Optimizing dosimetric accuracy for cancer treatment with flattened and flattening filter-free photon 6 megavoltage beams: Using GAMOS and GATE Monte Carlo codes

Ali H. D. Alshehri*

Department of Radiological Sciences, College of Applied Medical Sciences, Najran University, Najran, Saudi Arabia.

Abstract

This research investigates the optimization of cancer treatment by analyzing the dosimetric characteristics of 6 megavoltage flattened and flattening filter-free photon beams through detailed Monte Carlo simulations utilizing the GAMOS and GATE codes. Photon beams generated by a Varian medical linear accelerator were assessed based on critical factors such as dose rate, percentage depth doses(PDDs), out-of-field doses(OFDs), beam profiles scatter factor, energy spectrum, surface dose, and head and total scatter correction factor.

The results demonstrate that FFF beams, as modeled with GAMOS and GATE, provide a notably higher dose rate-approximately 2.3 times greater than that of FF beams-potentially leading to reduced treatment durations. Specifically, the dose rate for FFF beams was 3.8 Gy/min compared to 1.6 Gy/min for FF beams. Additionally, the FFF beams produced a 25.0% decrease in out-of-field dose(OFD) 3.5 cm away from the field edge, attributed to reduced head scatter. However, simulations also indicated increased surface and buildup doses for FFF beams, with surface doses being around 15% higher than FF beams. By substituting the air below the secondary collimator jaws of the linear accelerator with helium(He), the ratio of surface dose was reduced from 1.24 to 1.14, while the buildup dose and d_{max} values were brought back in line with those of FF beams.

This in-depth Monte Carlo analysis underscores the potential benefits of FFF beams in delivering more efficient radiation doses and lowering out-of-field exposure. Nonetheless, managing surface and build-up doses remains essential. With appropriate modifications, FFF technology could significantly enhance cancer treatment outcomes while reducing radiation exposure to surrounding healthy tissue, making it a promising tool for clinical use.

Keywords: PDD, FF/FFF beams, GAMOS/GATE Codes, Varian, HSCF, TSCF.

1. Introduction

Cancer remains one of the leading causes of death worldwide [Kastrati et al. (2021)], necessitating continuous advancements in treatment modalities [Grkovski et al. (2023); Spina and Chow (2022)]. Radiotherapy, particularly external beam radiotherapy (EBRT) [Fiak et al. (2021)], plays a crucial role in the management of various cancers, offering a non-invasive approach to tumor eradication [Javedan et al. (2014); Bhuiyan et al. (2022)]. Among the different types of radiation therapy [Adom et al. (2023)], photon beam therapy using lin-

*Corresponding author
Email address: ahzafer@nu.edu.sa (Ali H. D. Alshehri)

ear accelerators (linacs) has been a cornerstone due to its ability to deliver precise doses to target tissues while sparing surrounding healthy structures [Pawiro et al. (2020)]. However, the optimization of dose delivery is an ongoing challenge, requiring the careful balancing of treatment efficacy with the minimization of adverse effects [Xhafa et al. (2014); Capala et al. (2021)].

A significant factor influencing the dose distribution in photon beam therapy is the use of a flattening filter (FF) [Sadrollahi et al. (2019); Al-Zain et al. (2019)]. Traditionally, FFs have been incorporated into the linac beam path to produce a uniform dose distribution across the treatment field [Li et al. (2022)], particularly at a reference depth of 10.0 cm. While FFs achieve the desired beam flatness [Bilalodin and Abdullatif (2022)], they also introduce several drawbacks. The presence of an FF reduces the overall dose rate, increasing treatment times [Stanton and Stinson (1996); Bidmead et al. (1995)]. Furthermore, FFs contribute to scattered radiation, which can increase out-of-field doses and potentially impact healthy tissue adjacent to the treatment area [Podgorsak et al. (2003)]. These limitations have driven interest in unflattened (FFF) photon beams [Spina and Chow (2022)], which are increasingly being explored for their potential to enhance treatment efficiency and safety [Niemelä et al. (2017)]. The removal of the flattening filter from the linac beam path offers several potential advantages [Kastrati et al. (2021)]. FFF beams are characterized by a significantly higher dose rate [Mia et al. (2019)], which can reduce treatment times and improve patient throughput [Mott and West (2021)]. Additionally, the absence of the filter results in reduced head scatter [Majeed and Gupta (2020)], which lowers the out-of-field dose(OFD) and diminishes the radiation exposure to healthy tissues surrounding the tumor [Kim et al. (1991)]. However, FFF beams also present unique challenges, including increased surface and build-up doses [Rezzoug et al. (2023)], which must be carefully managed to avoid compromising the treatment's therapeutic ratio [Pawiro et al. (2020)].

Monte Carlo (MC) simulation using GAMOS and GATE Monte Carlo codes has emerged as a powerful tool for the detailed analysis of photon beam characteristics [Agostinelli et al. (2003)]. MC methods allow for precise modeling of complex radiation interactions within the linac head and patient tissues, providing invaluable insights into the dosimetric properties of both FF and FFF beams. By leveraging MC simulations, researchers can explore the impact of various beam configurations on dose distribution [Paelinck et al. (2005)], enabling the optimization of treatment plans for maximum therapeutic benefit. In this study, A comprehensive Monte Carlo analysis was performed using GAMOS and GATE Monte Carlo codes to compare the dosimetric characteristics of 6 megavoltage flattened(FF) and unflattened(FFF) photon beams [Al-Zain et al. (2019)] generated by a Varian linac [Rocha et al. (2022)]. Critical parameters such as percentage depth doses(PDDs), rate of dose, out-of-field doses (OFDs), beam profiles, energy spectrum, scatter factor, and surface dose were evaluated [Morias et al. (2018)]. The aim is to determine the potential advantages of FFF beams in optimizing cancer treatment, particularly in terms of improving dose delivery efficiency and minimizing exposure to surrounding healthy tissues [Bidmead et al. (1995)]. The findings from this analysis aim to contribute to the ongoing refinement of radiotherapy techniques, with the ultimate goal of enhancing treatment outcomes for cancer patients.

This investigation not only provides a detailed comparison of FF and FFF beams but also explores the practical implications of adopting FFF technology in clinical settings. By addressing both the benefits and challenges associated with FFF beams, It was sought to offer a balanced perspective that can inform future developments in photon beam therapy. In this study, the advancement of radiotherapy techniques that can provide

more precise, effective, and safer cancer treatments was supported, ultimately leading to improved patient care and outcomes.

2. Materials and Methods

This study investigates the dosimetric properties of a 6 megavoltage photon beam generated by a Varian medical linear accelerator [Morias et al. (2018)], utilizing the GAMOS and GATE Monte Carlo simulation codes [Arce et al. (2020); Al-Zain et al. (2019)]. The linac head geometry, including critical components such as the target, primary collimator [Hrbacek et al. (2011)], flattening filter, and jaws, was meticulously modeled following detailed specifications from Varian Medical Systems (Palo Alto, CA, USA). These elements are vital for shaping and delivering the photon beam, and their accurate configuration is crucial for precise simulations [Harkness et al. (2012)]. To ensure the accuracy of the simulations, the Monte Carlo models were rigorously validated against experimental data. Measurements were carried out using a $40 \times 40 \times 40$ cm^3 water phantom citeal2019validation, a standard medium for replicating human tissue in radiotherapy dosimetry [Bacala (2020)]. The phantom was placed at a source-to-surface distance(SSD) of 100.0 cm, a typical clinical setup for ensuring relevant and reproducible results [Abou-Shady et al. (2017)]. The data obtained from the water phantom were compared with the simulation results, providing a comprehensive assessment of the beam's dosimetric characteristics [Teixeira et al. (2019)].

2.1. Monte Carlo Simulations

The GAMOS and GATE codes were employed to simulate the photon interactions within the linac head and the water phantom [Arce et al. (2014); Gonias et al. (2016)]. These Monte Carlo codes are well-established in the field of radiotherapy for their ability to model complex radiation transport processes with high accuracy [Gasteuil et al. (2019)]. By simulating the beam's passage through the linac components and its subsequent interactions within the water phantom, the study aimed to replicate the actual dose distribution observed in clinical settings [Jin et al. (2016)].

2.2. Monte Carlo Validation

The Monte Carlo(MC) simulations were validated by comparing them with experimental measurements [Reynaert et al. (2007)]. These measurements were obtained using a $40 \times 40 \times 40$ cm^3 water phantom, positioned at a source-to-surface distance(SSD) of 100.0 cm. The experimental data, including dose distributions and beam profiles, were thoroughly compared with the simulated results to verify the accuracy of the models. Any observed discrepancies were carefully evaluated and corrected to improve the precision of the simulations [Witte and Sonke (2024)].

2.3. Dosimetric Properties Calculations

This study performed comprehensive calculations of essential dosimetric parameters for both flattened(FF) and unflattened(FFF) photon beams [Chen et al. (2005)]. Key metrics, including percentage depth dose(PDD)[Mesbahi and Zergoug (2015)], dose rate, scatter factor, and energy spectra, were analyzed to evaluate the beams' ability to deliver precise and effective radiation doses to the target region, while minimizing unnecessary exposure to adjacent healthy tissues. These calculations provide critical insights into optimizing beam performance for improved clinical outcomes [Ilias et al. (2013)].

2.4. PDDs, d_{max}, and Dose Rate

Percentage depth dose(PDD) curves were generated for various field sizes to assess how the dose changes with depth within the tissue [Zhang et al. (2016)]. The maximum dose depth (d_{max}) and dose rate were also calculated and compared between FF and FFF beams. These parameters are critical for understanding the beam's penetration and its ability to deliver the prescribed dose at different tissue depths [Şahmaran and Yılmaz Koca (2023)].

2.5. Beam Profiles and Out-of-Field Dose

The beam profiles were evaluated to assess the dose distribution across the treatment field at varying depths [Sadoughi et al. (2014)]. Both the uniformity of dose delivery and the characteristics of the penumbra were examined for Flattened (FF) and unflattened (FFF) beams [Spina and Chow (2022)]. In addition, the out-of-field dose was quantified, with particular attention to the reduced radiation delivered beyond the primary treatment field when using FFF beams, which is attributed to reduced head scatter. This analysis is critical for understanding the advantages of FFF beams in minimizing radiation exposure to healthy tissues surrounding the treatment area [Javedan et al. (2014)].

2.6. Surface Dose and Buildup

Surface dose and buildup regions were analyzed for both flattened and unflattened beams using different field size [Pawiro et al. (2020)]. The study focused on comparing the surface dose delivered to the skin or superficial tissues and examining the buildup region, where the dose rapidly increases to a maximum (d_{max}). The effects of removing the flattening filter on these parameters were evaluated, with special consideration given to modifications such as changing the air column under the secondary collimator jaws with helium(He).

2.7. Head and Total Scatter Correction Factor

The head scatter correction factor(HSCF) accounts for scatter from the linac head components [Almberg et al. (2012)], while the total scatter correction factor(TSCF) includes both head scatter and medium scatter. Using GAMOS and GATE Monte Carlo simulations, these factors were calculated for 6 megavoltage flattened(FF) and flattening filter-free(FFF) photon beams across different field sizes. The analysis helps evaluate the impact of the flattening filter on beam scatter, crucial for improving treatment accuracy [Jin et al. (2016)].

3. Results

The table 1 provides the D_{20}/D_{10} ratios for Flattened and unflattened 6 megavoltage photon beams at different field sizes from $5 \times 5\ cm^2$ to $20 \times 20\ cm^2$, as calculated using GAMOS and GATE codes for a Varian medical linear accelerator [Arce et al. (2020)].

For the $5 \times 5\ cm^2$ field size, the D_{20}/D_{10} ratios for FF beams are 0.55 with GAMOS and 0.56 with GATE, indicating a moderate dose gradient and relatively gradual dose fall-off [Harkness et al. (2012)]. In contrast, the FFF beams have slightly lower ratios of 0.52 for GAMOS and 0.53 for GATE, reflecting a steeper dose gradient and more pronounced dose fall-off at the edges. This result is expected given that FFF beams, lacking a flattening filter, have a more pronounced central dose peak and a more rapid dose decrease at the periphery. At the $10 \times 10\ cm^2$ field size, the D_{20}/D_{10} ratios for FF beams increase to 0.57 (GAMOS) and 0.58 (GATE), showing a slightly larger dose gradient compared to the smaller field size. This suggests that while FF beams

continue to offer reasonable dose uniformity in medium-sized fields, the dose fall-off becomes more noticeable. For FFF beams, the ratios are 0.54 (GAMOS) and 0.55 (GATE), indicating a more pronounced dose gradient and sharper dose fall-off compared to FF beams, consistent with the effects observed in larger fields. For the $20 \times 20\ cm^2$ field size, the D_{20}/D_{10} ratios for FF beams further increase to 0.61 (GAMOS) and 0.62 (GATE), reflecting a broader dose fall-off region. This increase highlights the challenge of maintaining dose uniformity in larger fields with FF beams. In comparison, the FFF beams exhibit ratios of 0.57 (GAMOS) and 0.58 (GATE), showing a significant dose gradient at the edges of the large field [Al-Zain et al. (2019)]. The absence of the FF in FFF beams results in a sharper dose fall-off, which becomes more pronounced as the field size increases [Spina and Chow (2022)].

Moreover, the D_{20}/D_{10} ratios indicate that FF beams generally provide a more gradual dose fall-off, leading to better dose uniformity across various field sizes. In contrast, FFF beams, while advantageous for high-dose treatments in smaller fields, exhibit a steeper dose gradient and more pronounced dose fall-off in larger fields [Javedan et al. (2014)]. The choice between FF and FFF beams should be guided by the clinical requirements, considering the trade-off between dose uniformity and dose delivery efficiency.

Table 1: Ratios of D_{20}/D_{10} for different field sizes of 6 megavoltage Flattened(FF) and unflattened(FFF) photon beams at a 10.0 cm depth, calculated using GAMOS and GATE Monte Carlo(MC) simulations for a Varian medical linear accelerator.

Field Size (cm^2)	**Flattened (FF)**		**Unflattened (FFF)**	
	GAMOS	GATE	GAMOS	GATE
5×5	0.55	0.56	0.52	0.53
10×10	0.57	0.58	0.54	0.55
20×20	0.61	0.62	0.57	0.58

The analysis of D_{max}/D_{min} ratios for 6 megavoltage photon beams using Flattened and unflattened configurations reveals significant insights into dose distribution characteristics at different field sizes of [$5 \times 5\ cm^2$, $10 \times 10\ cm^2$, and $20 \times 20\ cm^2$], calculated at a depth of 10.0 cm using GAMOS and GATE codes for a Varian medical linear accelerator.

For the $5 \times 5\ cm^2$ field size, both Flattened(FF) and unflattened (FFF) beams exhibit minimal dose variation within 80% of the field size, with D_{max}/D_{min} ratios of 1.01 for FF beams and slightly higher values for FFF beams (1.06 with GAMOS and 1.05 with GATE). This reflects that in the small field size, FF beams maintain nearly uniform dose distribution, while FFF beams show a modest increase in dose variation due to the absence of the flattening filter, resulting in a more concentrated central dose and a more pronounced dose gradient at the periphery [Bilalodin and Abdullatif (2022)]. As the field size increases to $10 \times 10\ cm^2$, the FF beams continue to show a stable dose distribution with D_{max}/D_{min} ratios remaining at 1.01 for both GAMOS and GATE. In contrast, FFF beams exhibit increased dose variation, with ratios rising to 1.13 (GAMOS) and 1.12 (GATE). This increase indicates that the larger field size exacerbates the dose gradient effects of the FFF beams, leading to more noticeable dose variation compared to FF beams. For the $20 \times 20\ cm^2$ field size, FF beams maintain excellent

dose uniformity with ratios of 1.01 for both GAMOS and GATE. However, the FFF beams show a significant increase in dose variation, with ratios reaching 1.32 (GAMOS) and 1.30 (GATE), as shown in the table 2. This substantial rise highlights the impact of the absence of the flattening filter, which results in a pronounced central dose peak and a steeper dose fall-off at the field edges, leading to greater dose variability in larger fields [Stanton and Stinson (1996)].

Table 2: Ratios of the maximum dose (D_{max}) to the minimum dose (D_{min}) within 80 % of the field size for Flattened(FF) and Unflattened(FFF) 6 megavoltage photon beams at a depth of 10 cm, using GAMOS and GATE codes for a Varian medical linear accelerator.

Field Size (cm^2)	**Flattened (FF)**		**Unflattened (FFF)**	
	GAMOS	GATE	GAMOS	GATE
5×5	1.012	1.022	1.061	1.055
10×10	1.013	1.023	1.131	1.132
20×20	1.012	1.022	1.320	1.305

In this study, the comparison of percentage depth doses (PDDs) for unflattened(FFF) and flattened(FF) 6 megavoltage photon beams was performed using both measurements (for FF) and Monte Carlo simulations (GAMOS and GATE codes) in a water phantom for field sizes of [5×5 cm^2, 10×10 cm^2, and 20×20 cm^2]. The results showed that FFF beams delivered higher surface and build-up doses compared to FF beams due to the absence of the flattening filter, which reduces scatter. For all field sizes, the PDDs curves of the FFF beams exhibited steeper dose fall-off beyond the maximum depth (d_{max}), leading to a reduced dose at deeper tissues. In contrast, the FF beams showed a more gradual dose decrease with depth, reflecting the impact of beam flattening. The simulations using GAMOS and GATE codes closely matched the measured PDDs for FF beams, confirming the accuracy of the Monte Carlo models [Podgorsak et al. (2003)]. For FFF beams, the simulations consistently predicted higher dose rates at shallow depths, in agreement with experimental observations [Mia et al. (2019)]. These findings highlight the dosimetric benefits of FFF beams, particularly in decreasing treatment time and sparing deeper healthy tissues [Niemelä et al. (2017)], as seen in Figures 1.

In the Figures 1, comparison of beam profiles between flattened and unflattened 6 megavoltage photon beams for field sizes from 5×5 cm^2 to 20×20 cm^2] using GAMOS and GATE codes demonstrates significant variations in dose distributions. For smaller field sizes [5×5 cm^2], the FFF beam shows a sharper dose peak at the central axis with a faster dose fall-off towards the periphery, while the FF beam exhibits a more uniform dose distribution. As field size increases [10×10 cm^2 and 20×20 cm^2], this trend persists, with the FFF beam consistently showing higher central axis dose and reduced penumbra compared to the FF beam [Kastrati et al. (2021)]. GAMOS and GATE simulations closely align with measured data for FF beams, confirming the accuracy of the Monte Carlo models. However, the FFF beams result in lower out-of-field doses due to the absence of scattering from the flattening filter. The slight discrepancies between simulations and measurements in penumbra regions are likely due to limitations in modeling secondary scatter [Kim et al. (1991)]. Overall, these results suggest that FFF beams offer dosimetric advantages in high-precision radiotherapy, particularly for smaller fields.

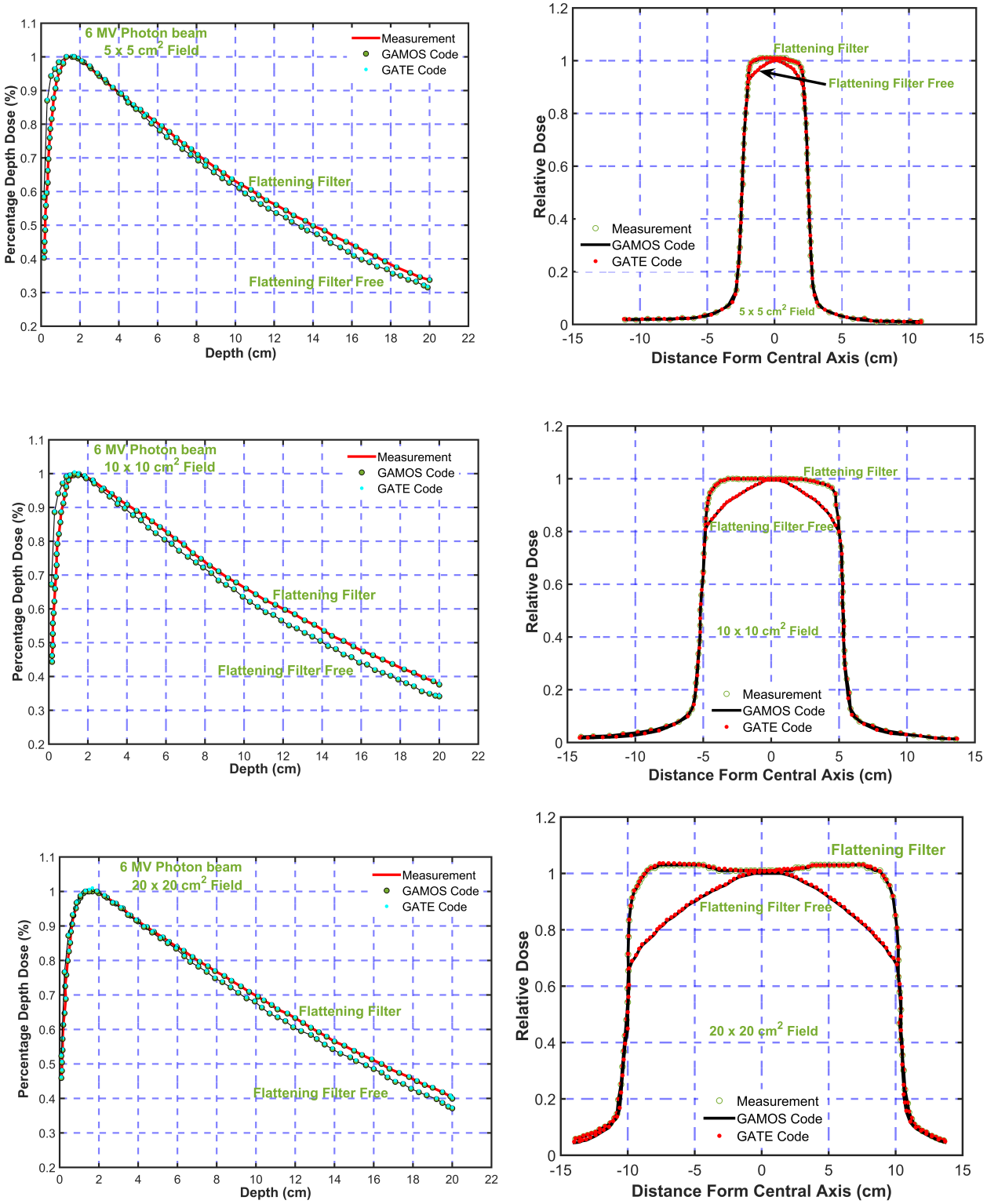

Figure 1: Comparison of Percentage Depth Doses(PDDs) and Photon Beam Spectra for and Flattened(FF) and Unflattened(FFF) 6 megavoltage Photon Beams Across [$5 \times 5\ cm^2$, $10 \times 10\ cm^2$, and $20 \times 20\ cm^2$] Field Sizes: Experimental Measurements for FF Beams and Monte Carlo Simulations Using GAMOS and GATE Codes.

In this work, the photon energy spectra of flattened and unflattened 6 megavoltage photon beams were compared for field sizes from $5 \times 5\ cm^2$ to $20 \times 20\ cm^2$ using GAMOS and GATE Monte Carlo codes. The results revealed notable differences in the energy spectra between flattened and unflattened beams across all field sizes.

For the FFF beams, the spectra were generally softer, with a higher proportion of lower-energy photons due to the absence of the flattening filter, which typically hardens the beam by attenuating lower-energy photons [Rezzoug et al. (2023)]. In contrast, the FF beams displayed a more uniform and hardened spectrum, especially in larger field sizes. The softening of the FFF beam spectrum was more pronounced at smaller field sizes (5×5 cm^2), while the difference decreased with increasing field size (20×20 cm^2). Monte Carlo simulations using both GAMOS and GATE codes closely aligned with experimental data, accurately reflecting the impact of the flattening filter on the energy spectra. These differences in photon spectra between FF and FFF beams contribute to variations in dose distribution and out-of-field dose [Paelinck et al. (2005)], highlighting the potential advantages of FFF beams in certain radiotherapy applications, as seen in Figures 2.

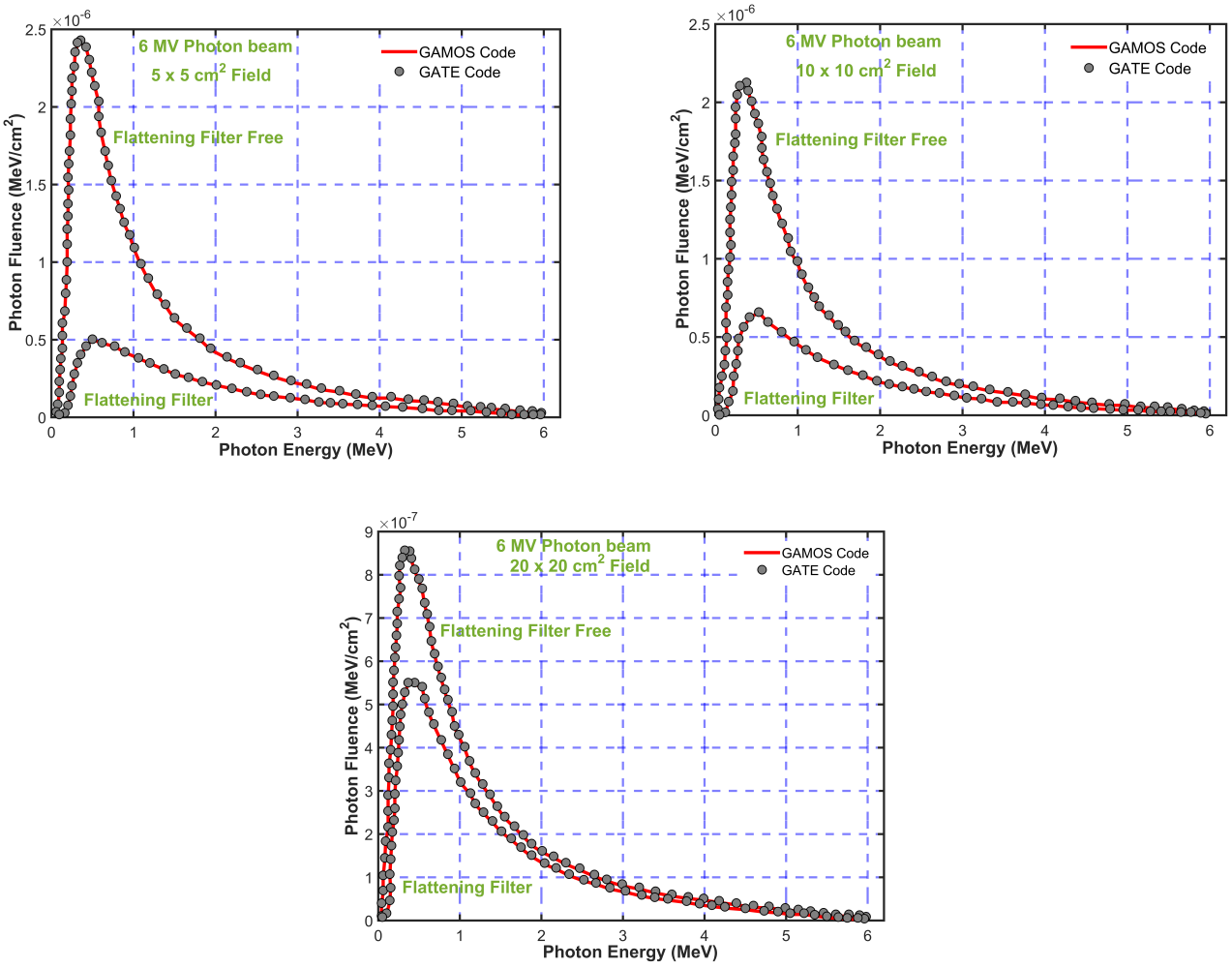

Figure 2: A comparative analysis of photon beam spectra for 6 megavoltage Flattened(FF) and unflattened(FFF) photon beams across field sizes of [5×5 cm^2, 10×10 cm^2, and 20×20 cm^2], obtained using GAMOS and GATE Monte Carlo simulations.

The results obtained from the Monte Carlo(MC) simulations using GAMOS and GATE codes demonstrate differences between the dosimetric characteristics of 6 megavoltage flattened(FF) and unflattened(FFF) photon beams [Morias et al. (2018)]. The Total Scatter Correction Factor (TSCF) and Head Scatter Correction Factor (HSCF) show distinct patterns, which highlight the advantages and limitations of both beam types. For all field sizes, the TSCF is higher for FF beams compared to FFF beams. This is expected due to the scattering introduced by the flattening filter, which interacts with the primary photon beam and contributes additional scatter

within the treatment field and beyond. As the field size increases, the TSCF values also rise for both beam types, reflecting the increased scatter contributions from the larger volume of tissue irradiated [Rocha et al. (2022)]. However, FFF beams consistently show lower TSCF values, indicating less scatter and a more concentrated dose distribution, which is favorable for reducing unwanted radiation to healthy tissues. The HSCF follows a similar trend, with higher values observed for FF beams across all field sizes. The presence of the flattening filter significantly increases head scatter by interacting with primary photons and generating secondary scatter. This effect is especially pronounced in larger fields where the photon scatter from the linac head components is more substantial. On the other hand, FFF beams, which eliminate the flattening filter, demonstrate a considerable reduction in head scatter, as shown by the lower HSCF values. This reduction in scatter is particularly advantageous for modern radiotherapy techniques that prioritize dose precision [Bidmead et al. (1995)], such as intensity-modulated radiotherapy(IMRT)[Reynaert et al. (2007)] and stereotactic body radiotherapy(SBRT)[Hrbacek et al. (2011)], as seen in Figures 3 and 4.

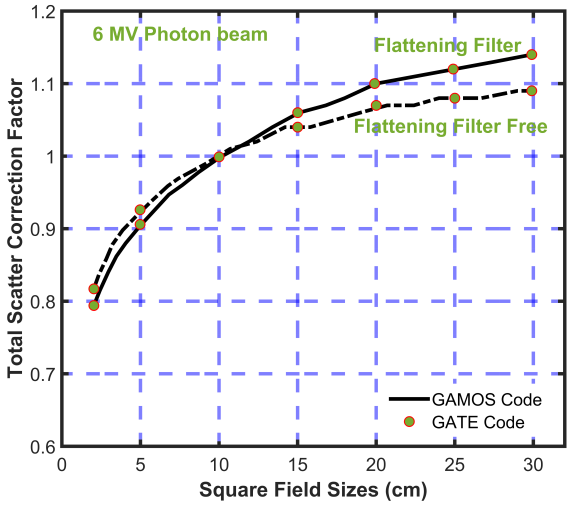

Figure 3: A comparison of the total scatter correction factor(TSCF) curves along the lateral sides of the irradiation field for Flattened and unflattened 6 megavoltage photon beams across various square field sizes of [5×5 cm^2, 10×10 cm^2, and 20×20 cm^2], obtained using GAMOS and GATE Monte Carlo simulations.

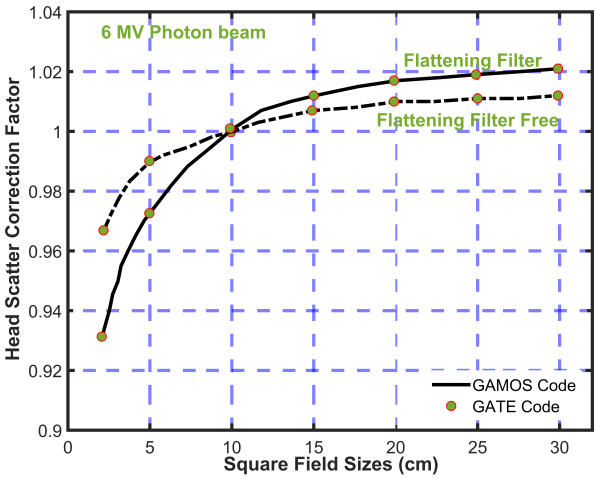

Figure 4: A comparison of the head scatter correction factor(HSCF) curves along the lateral sides of the irradiation field for Flattened and unflattened 6 megavoltage photon beams across various square field sizes of [5×5 cm^2, 10×10 cm^2, and 20×20 cm^2], obtained using GAMOS and GATE Monte Carlo simulations.

One of the key findings is the potential clinical benefit of FFF beams. The increased dose rate associated with FFF beams can significantly shorten treatment times, improving patient comfort and reducing the likelihood of motion artifacts during treatment. Additionally, the reduced out-of-field dose(OFD) for FFF beams, resulting from lower head scatter, minimizes radiation exposure to surrounding healthy tissues, enhancing the safety profile of FFF-based treatments. However, the higher surface and buildup doses associated with FFF beams present a challenge. These effects, while manageable, require careful consideration in treatment planning, especially for patients with tumors located near sensitive structures. Interestingly, the study found that changing the air column under the linac jaws with helium mitigated some of these effects, restoring dose characteristics closer to those of FF beams.

Faintly, the results indicate that FFF beams provide distinct dosimetric advantages, including higher dose

rates, reduced scatter, and lower out-of-field doses. These features make FFF beams a promising option for advanced radiotherapy techniques, though careful management of surface and buildup doses remains essential.

4. Conclusion

This study presents a comprehensive analysis of the dosimetric characteristics of 6 megavoltage flattened (FF) and unflattened(FFF) photon beams generated by a Varian medical linear accelerators (LINAC), using GAMOS and GATE Monte Carlo simulations. The results demonstrate that FFF beams offer significant advantages, including increased dose rates and decreased out-of-field doses(OFDs), which can lead to shorter treatment times and reduced exposure to healthy tissue. While FFF beams exhibit higher surface and buildup doses, these can be mitigated by adjusting the treatment setup, such as introducing helium to reduce surface dose. The detailed comparison of photon energy spectra, beam profiles, and percentage depth doses (PDDs) confirms the clinical viability of FFF beams, particularly for modern radiotherapy techniques such as IMRT and SBRT. This study underscores the potential of FFF beams to enhance therapeutic outcomes while maintaining safety, making them a promising option for optimizing cancer treatment in the clinical setting.

Acknowledgment

The author is thankful to the Deanship of Scientific Research at Najran University for funding this work under the Easy Research Funding Program. "grant code will be provided later"

References

Abou-Shady, H., Hozayed, S., Ibrahim, H., 2017. Design and modeling of medical linear accelerators using the geant4/gate platform. Journal of Nuclear Technology in Applied Science 5, 241. URL: https://inis.iaea.org/search/search.aspx?orig_q=RN:49079968.

Adom, J., Addison, E.K., Awuah, B.K., Hasford, F., Owusu-Mensah, M., 2023. Towards clinical use of varian clinac ix linear accelerator in a low resource radiotherapy facility: evaluation of commissioning data. Health and Technology 13, 571–583. URL: https://doi.org/10.1007/s12553-023-00769-9.

Agostinelli, S., Allison, J., Amako, K.a., Apostolakis, J., Araujo, H., Arce, P., Asai, M., Axen, D., Banerjee, S., Barrand, G., et al., 2003. Geant4-a simulation toolkit. Nuclear instruments and methods in physics research section A: Accelerators, Spectrometers, Detectors and Associated Equipment 506, 250–303. URL: https://doi.org/10.1016/S0168-9002(03)01368-8.

Al-Zain, J., El Bardouni, T., Mohammed, M., El Hajjaji, O., 2019. Validation of gamos code based on geant4 monte carlo for a 12 mv saturne43 linac. Journal of King Saud University-Science 31, 500–505. URL: https://doi.org/10.1016/j.jksus.2018.07.003.

Almberg, S., Frengen, J., Lindmo, T., 2012. Monte carlo study of in-field and out-of-field dose distributions from a linear accelerator operating with and without a flattening-filter. Medical physics 39, 5194–5203. URL: https://doi.org/10.1118/1.4738963.

Arce, P., Lagares, J.I., Azcona, J.D., Aguilar-Redondo, P.B., 2020. A proposal for a geant4 physics list for radiotherapy optimized in physics performance and cpu time. Nuclear Instruments and Methods in Physics Research Section A: Accelerators, Spectrometers, Detectors and Associated Equipment 964, 163755. URL: https://doi.org/10.1016/j.nima.2020.163755.

Arce, P., Lagares, J.I., Harkness, L., Pérez-Astudillo, D., Cañadas, M., Rato, P., de Prado, M., Abreu, Y., de Lorenzo, G., Kolstein, M., et al., 2014. Gamos: A framework to do geant4 simulations in different physics fields with an user-friendly interface. Nuclear Instruments and Methods in Physics Research Section A: Accelerators, Spectrometers, Detectors and Associated Equipment 735, 304–313. URL: https://doi.org/10.1016/j.nima.2013.09.036.

Bacala, A.M., 2020. Linac photon beam fine-tuning in primo using the gamma-index analysis toolkit. Radiation Oncology 15, 1–11. URL: https://doi.org/10.1186/s13014-019-1455-1.

Bhuiyan, M., Chen, C.T., Freifelder, R., Zhang, H., Meier, J., Tsai, H.M., Kao, C.M., Raubic, A.K., Nolen, J., Rotsch, D., et al., 2022. Targeting muc1-c for cancer theranostics using humanized 47sc-mab 3d1. URL: https://jnm.snmjournals.org/content/63/supplement_2/2357.

Bidmead, A., Garton, A., Childs, P., 1995. Beam data measurements for dynamic wedges on varian 600c (6 mv) and 2100c (6 and 10 mv) linear accelerators. Physics in Medicine & Biology 40, 393. URL: https://doi.org/10.1088/0031-9155/40/3/005.

Bilalodin, B., Abdullatif, F., 2022. Modeling and analysis of percentage depth dose (pdd) and dose profile of x-ray beam produced by linac device with voltage variation. Jurnal Ilmiah Teknik Elektro Komputer dan Informatika (JITEKI) 8, 206–214. URL: https://doi.org/10.26555/jiteki.v8i2.23622.

Capala, J., Graves, S.A., Scott, A., Sgouros, G., James, S.S., Zanzonico, P., Zimmerman, B.E., 2021. Dosimetry for radiopharmaceutical therapy: current practices and commercial resources. Journal of Nuclear Medicine 62, 3S–11S. URL: https://doi.org/10.2967/jnumed.121.262749.

Chen, X., Yue, N.J., Chen, W., Saw, C.B., Heron, D.E., Stefanik, D., Antemann, R., Huq, M.S., 2005. A dose verification method using a monitor unit matrix for dynamic imrt on varian linear accelerators. Physics in Medicine & Biology 50, 5641. URL: http://dx.doi.org/10.1088/0031-9155/50/23/016.

Fiak, M., Fathi, A., Inchaouh, J., Khouaja, A., Benider, A., Krim, M., Harakat, N., Housni, Z., Bouhssa, M., Mouadil, M., et al., 2021. Monte carlo simulation of a 18 mv medical linac photon beam using gate/geant4. Moscow University Physics Bulletin 76, 15–21. URL: https://doi.org/10.3103/S0027134921010069.

Gasteuil, J., Noblet, C., Moreau, M., Meyer, P., 2019. A gate/geant4 monte carlo toolkit for surface dose calculation in vmat breast cancer radiotherapy. Physica Medica 61, 112–117. URL: https://doi.org/10.1016/j.ejmp.2019.04.012.

Gonias, P., Zaverdinos, P., Loudos, G., Kappas, C., Theodorou, K., 2016. Monte carlo simulation of a 6 mv varian linac photon beam using geant4-gate code. Physica Medica 32, 333. URL: https://doi.org/10.1016/j.ejmp.2016.07.245.

Grkovski, M., O'Donoghue, J.A., Imber, B.S., Andl, G., Tu, C., Lafontaine, D., Schwartz, J., Thor, M., Zelefsky, M.J., Humm, J.L., et al., 2023. Lesion dosimetry for [177lu] lu-psma-617 radiopharmaceutical therapy combined with stereotactic body radiotherapy in patients with oligometastatic castration-sensitive prostate cancer. Journal of Nuclear Medicine 64, 1779–1787. URL: https://doi.org/10.2967/jnumed.123.265763.

Harkness, L., Arce, P., Judson, D., Boston, A., Boston, H., Cresswell, J., Dormand, J., Jones, M., Nolan, P., Sampson, J., et al., 2012. A compton camera application for the gamos geant4-based framework. Nuclear Instruments and Methods in Physics Research Section A: Accelerators, Spectrometers, Detectors and Associated Equipment 671, 29–39. URL: https://doi.org/10.1016/j.nima.2011.12.058.

Hrbacek, J., Lang, S., Klöck, S., 2011. Commissioning of photon beams of a flattening filter-free linear accelerator and the accuracy of beam modeling using an anisotropic analytical algorithm. International Journal of Radiation Oncology* Biology* Physics 80, 1228–1237. URL: https://doi.org/10.1016/j.ijrobp.2010.09.050.

Ilias, A., Diallo, I., Bezin, J., 2013. Modeling in the leakage radiation of a medical linear accelerator a function of the collimator opening: analytical extrapolation of the leak field opened by a method semi-empirical based measurement at zero field. Physica Medica 29, e23. URL: https://doi.org/10.1016/j.ejmp.2013.08.073.

Javedan, K., Feygelman, V., Zhang, R.R., Moros, E.G., Correa, C.R., Trotti, A., Li, W., Zhang, G.G., 2014. Monte carlo comparison of superficial dose between flattening filter free and flattened beams. Physica medica 30, 503–508. URL: https://doi.org/10.1016/j.ejmp.2014.03.001.

Jin, S., Wang, K., Fan, Y., Wang, Z., Huang, J., Yang, X., Zhang, J., 2016. The reproduction for the absorbed-dose to water of the clinical accelerator photon beams. Physica Medica 32, 265–266. URL: https://doi.org/10.1016/j.ejmp.2016.07.577.

Kastrati, L., Hodolli, G., Kadiri, S., Demirel, E., Istrefi, L., Kabashi, Y., Uka, B., 2021. Applications and benefits of using gradient percentage depth dose instead of percentage depth dose for electron and photon beams in radiotherapy. Polish Journal of Medical Physics and Engineering 27, 25–29. URL: https://doi.org/10.2478/pjmpe-2021-0004.

Kim, K.J., Lee, J.Y., Park, K.R., 1991. Characteristics of 15 mv photon beam from a varian clinac 1800 dual energy linear accelerator. Radiation Oncology Journal 9, 131–141.

Li, Y., Sun, X., Liang, Y., Hu, Y., Liu, C., 2022. Monte carlo simulation of linac using primo. Radiation Oncology 17, 185. URL: https://doi.org/10.1186/s13014-022-02149-5.

Majeed, H., Gupta, V., 2020. Adverse effects of radiation therapy URL: https://www.ncbi.nlm.nih.gov/books/NBK563259/.

Mesbahi, A., Zergoug, I., 2015. Dose calculations for lung inhomogeneity in high-energy photon beams and small beamlets: a comparison between xio and tigrt treatment planning systems and mcnpx monte carlo code. Iranian Journal of Medical Physics 12, 167–77. URL: https://doi.org/10.22038/IJMP.2015.6218.

Mia, M., Rahman, M., Purohit, S., Kabir, S., Meaze, A., 2019. Analysis of percentage depth dose for 6 and 15 mv photon energies of medical linear accelerator with cc13 ionization chamber. Nuclear Science and Applications 28.

Morias, S., Marcu, L.G., Short, M., Giles, E., Potter, A., Shepherd, J., Gierlach, T., Bezak, E., 2018. Treatment-related adverse effects in lung cancer patients after stereotactic ablative radiation therapy. Journal of oncology 2018, 6483626. URL: https://doi.org/10.1155/2018/6483626.

Mott, J., West, N., 2021. Essentials of depth dose calculations for clinical oncologists. Clinical Oncology 33, 5–11. URL: https://doi.org/10.1016/j.clon.2020.06.021.

Niemelä, J., Partanen, M., Ojala, J., Sipilä, P., Björkqvist, M., Kapanen, M., Keyriläinen, J., 2017. Measurement and properties of the dose–area product ratio in external small-beam radiotherapy. Physics in Medicine & Biology 62, 4870. URL: https://doi.org/10.1088/1361-6560/aa6861.

Paelinck, L., De Wagter, C., Van Esch, A., Duthoy, W., Depuydt, T., De Neve, W., 2005. Comparison of build-up dose between elekta and varian linear accelerators for high-energy photon beams using radiochromic film and clinical implications for imrt head and neck treatments. Physics in Medicine & Biology 50, 413. URL: https://doi.org/10.1088/0031-9155/50/3/002.

Pawiro, S., Azzi, A., Soejoko, D., 2020. A monte carlo study of photon beam characteristics on various linear accelerator filters. Journal of Biomedical Physics & Engineering 10, 613. URL: https://doi.org/10.31661/jbpe.v0i0.1192.

Podgorsak, E.B., et al., 2003. Review of radiation oncology physics: a handbook for teachers and students. Vienna, Austria: IAE Agency 19, 133. URL: https://doi.org/10.1038/sj.bjc.6604224.

Reynaert, N., Van der Marck, S., Schaart, D., Van der Zee, W., Van Vliet-Vroegindeweij, C., Tomsej, M., Jansen, J., Heijmen, B., Coghe, M., De Wagter, C., 2007. Monte carlo treatment planning for photon and electron beams. Radiation Physics and Chemistry 76, 643–686. URL: https://doi.org/10.1016/j.radphyschem.2006.05.015.

Rezzoug, M., Zerfaoui, M., Oulhouq, Y., Rrhioua, A., Didi, S., Hamal, M., Moussa, A., 2023. Varian clinac 2100 linear accelerator simulation employing primo phase space model. Radiation Physics and Chemistry 207, 110859. URL: https://doi.org/10.1016/j.radphyschem.2023.110859.

Rocha, P.H., Reali, R.M., Decnop, M., Souza, S.A., Teixeira, L.A., Júnior, A.L., Sarpi, M.O., Cintra, M.B., Pinho, M.C., Garcia, M.R., 2022. Adverse radiation therapy effects in the treatment of head and neck tumors. RadioGraphics 42, 806–821. URL: https://doi.org/10.1148/rg.210150.

Sadoughi, H.R., Nasseri, S., Momennezhad, M., Sadeghi, H.R., Bahreyni-Toosi, M.H., 2014. A comparison between gate and mcnpx monte carlo codes in simulation of medical linear accelerator. Journal of Medical Signals & Sensors 4, 10–17. URL: https://journals.lww.com/jmss/fulltext/2014/04010/A_Comparison_Between_GATE_and_MCNPX_Monte_Carlo.2.aspx.

Sadrollahi, A., Nuesken, F., Licht, N., Rübe, C., Dzierma, Y., 2019. Monte-carlo simulation of the siemens artiste linear accelerator flat 6 mv and flattening-filter-free 7 mv beam line. PLoS One 14, e0210069. URL: https://doi.org/10.1371/journal.pone.0210069.

Şahmaran, T., Yılmaz Koca, C., 2023. Evaluation of dosimetric parameters after electron gun and ion pump replacement in linear accelerator device and comparison of results by gate/geant4 simulation. Radiation Effects and Defects in Solids 178, 1097–1108. URL: https://doi.org/10.1080/10420150.2023.2222328.

Spina, A., Chow, J.C., 2022. Dosimetric impact on the flattening filter and addition of gold nanoparticles in radiotherapy: a monte carlo study on depth dose using the 6 and 10 mv fff photon beams. Materials 15, 7194. URL: https://doi.org/10.3390/ma15207194.

Stanton, R., Stinson, D., 1996. Applied physics for radiation oncology. Medical Physics Publishing Corporation. URL: https://doi.org/10.54947/9781930524408.

Teixeira, M., Batista, D., Braz, D., Da Rosa, L., 2019. Monte carlo simulation of novalis classic 6 mv accelerator using phase space generation in gate/geant4 code. Progress in Nuclear Energy 110, 142–147. URL: https://doi.org/10.1016/j.pnucene.2018.09.004.

Witte, M., Sonke, J.J., 2024. A deep learning based dynamic arc radiotherapy photon dose engine trained on monte carlo dose distributions. Physics and Imaging in Radiation Oncology 30, 100575. URL: https://doi.org/10.1016/j.phro.2024.100575.

Xhafa, B., Mulaj, T., Hodolli, G., Nafezi, G., 2014. Dose distribution of photon beam by siemens linear accelerator. International Journal of Medical Physics, Clinical Engineering and Radiation Oncology 2014. URL: https://doi.org/10.4236/ijmpcero.2014.31011.

Zhang, Y., Feng, Y., Ming, X., Deng, J., 2016. Energy modulated photon radiotherapy: a monte carlo feasibility study. BioMed Research International 2016, 7319843. URL: http://dx.doi.org/10.1155/2016/7319843.